Available online at www.sciencedirect.com
SCIENCE DIRECT®
Journal of Organometallic Chemistry 690 (2005) 3027–3032
Journal of Organometallic Chemistry
www.elsevier.com/locate/jorganchem

Anodic polymerization of dithienosilole and electroluminescent properties of the resulting polymer

Joji Ohshita *, Daisuke Hamamoto, Keisuke Kimura, Atsutaka Kunai *

Department of Applied Chemistry, Graduate School of Engineering, Hiroshima University, 1-4-1 Kagamiyama, Higashi-Hiroshima 739-8527, Japan

Received 18 December 2004; revised 22 March 2005; accepted 22 March 2005
Available online 5 May 2005

Abstract

Anodic oxidation of 2,6-bis(trimethylsilyl)-4,4-di(*p*-tolyl)dithienosilole gave a dark orange solid polymer with a small band gap. The spectral analysis of the polymer indicated that decomposition of the dithienosilole ring system had competed the polymerization to an extent. This, however, could be suppressed by optimizing the reaction conditions. Applications of the spin-coated polymer films to electroluminescent materials are described.

Keywords: Silole; Anodic polymerization; Polythiophene; EL device

1. Introduction

A current interest has been focused on a silole (silacyclopentadiene) ring system, because of its low-lying LUMO energy level that originates the high electron affinity of silole-containing compounds [1,2]. Inclusion of a silole unit as a component of π-conjugated polymers and oligomers also has been studied, such as for example, by transition metal catalyzed cross-coupling reactions of 2,5-bifunctionalized siloles with carbon-based conjugated monomers [3], and oxidative coupling of dilithiosiloles [4]. Although electrochemical oxidation of heteroaromatic compounds, including thiophenes and pyrroles, has been extensively studied as a direct method to prepare π-conjugated polymers, only a little is known for anodic properties of siloles. Becker and his coworkers [5] reported that 2,3,4,5-tetraphenylsilole derivatives underwent decomposition of the silole ring system on electrochemical oxidation. In contrast to this, it was reported that anodic oxidation of 2,5-bis(3,4-ethylenedioxythienyl)silole produced silole-containing polymeric materials by the thiophene–thiophene oxidative coupling [6].

Recently, we reported the synthesis of dithienosiloles (DTSs) that have a silole system fused with two thiophene rings [7]. Like other silole-containing compounds, DTSs have low-lying LUMO and may be used as the electron-transport for electroluminescent devices [7–9]. They are electrochemically active and the cyclic voltammograms (CVs) revealed an irreversible anodic peak. However, anodic polymerization of DTSs by using repeated potential scan in 0.1 M $LiClO_4$–acetonitrile (AN) did not give expected poly(DTSs), but produced only polythiophene-like polymers with liberation of organosilicon moieties [7]. In this paper, we report anodic polymerization of DTS **1** by applying a constant potential to AN solutions of **1** containing Et_4NBF_4 as a supporting electrolyte, which produced polymer **2** having DTS units remaining in the backbone to a large extent (Scheme 1).

* Corresponding authors. Tel.: +81824247743; fax: +81824245494 (Joji Ohshita).
E-mail address: jo@hiroshima-u.ac.jp (J. Ohshita).

0022-328X/$ - see front matter © 2005 Elsevier B.V. All rights reserved.
doi:10.1016/j.jorganchem.2005.03.039

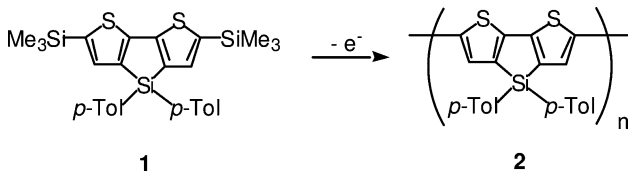

1 2

Scheme 1. Synthesis of polymer **2**.

2. Experimental

The starting DTS **1** was prepared as reported in the literature [7]. Poly(3-hexylthiophene) (**7**), having head-to-tail linkage >97%, was purchased from Aldrich Chemical Co. and used as obtained. Acetonitrile was distilled two times from KOH and stored in a sealed ample at −20 °C until use. Molecular weights of polymer **2** were determined by GPC, using THF as the eluent, and are relative to polystyrene standards.

Electrolysis of **1** was carried out in AN containing 0.05–0.2 M of an electrolyte, using Pt plates as working and counter electrodes. After electrolysis, the resulting red brown precipitates were collected and washed with AN. The precipitates were dissolved in chloroform and the insoluble substances were removed by filtration. Evaporation of the solvent under reduced pressure gave polymer **2** that was subjected to spectroscopic analysis. Optical properties and molecular weights of the polymers from several runs are summarized in Table 1. Data for polymer **2** obtained from run 7 in Table 1: ^{1}H NMR ($CDCl_3$) δ 0.26–0.32 (m, relative integration 1), 2.35 (br s, 6.1), 6.93–7.38 (m, 4.6), 7.41–7.61 (m, 5.4) (see Fig. 1).

Compounds **3** and **4** were separated from AN soluble part by preparative GPC eluting with benzene (Table 1, runs 1 and 2). Data for **3**: MS *m*/*z* 446 (M^+). ^{1}H NMR ($CDCl_3$) δ 0.33 (s, 9H), 2.35 (s, 6H), 7.04–7.35 (m, 7H), 7.54 (d, J = 7.7 Hz, 4H). ^{13}C NMR ($CDCl_3$) δ 0.1, 21.6, 125.9, 128.4, 129.0, 129.7, 135.5, 136.5, 140.3, 140.5, 141.7, 141.9, 150.2, 155.4. ^{29}Si NMR ($CDCl_3$) δ −21.5, −6.8. Anal. Calc. for $C_{25}H_{26}S_2Si_2$: C, 67.21; H, 5.87. Found: C, 67.00; H, 5.85%. Data for **4**: MS *m*/*z* 374 (M^+). ^{1}H NMR ($CDCl_3$) δ 2.34 (s, 6H), 7.13–7.21 (m, 6H), 7.25 (d, J = 5.6 Hz, 2H), 7.52 (d, J = 8.0 Hz, 4H). ^{13}C NMR ($CDCl_3$) δ 21.6, 125.7, 128.2, 129.0, 129.6, 135.4, 140.2, 140.3, 150.1; ^{29}Si NMR ($CDCl_3$) δ −20.9. Exact MS Calc. for $C_{22}H_{18}S_2Si$: 374.0608. Found: 374.0618.

Compounds **5** and **6** were isolated from the AN soluble parts from several runs, which were combined and treated with preparative GPC. Data for **5**: MS *m*/*z* 388 (M^+); ^{1}H NMR ($CDCl_3$) δ 0.10 (s, 18H), 2.35 (s, 6H), 7.15 (d, J = 8.0 Hz, 4H), 7.46 (d, J = 8.0 Hz, 4H). ^{29}Si NMR ($CDCl_3$) δ 9.20. Anal. Calc. for $C_{20}H_{32}0_2Si_3$: C, 61.80; H, 8.30. Found: C, 62.08; H, 8.14%. Data for **6**: MS *m*/*z* 464 (M^+). ^{1}H NMR ($CDCl_3$) δ −0.06 (s, 9H), 2.20 (s, 6H), 6.80 (dd, J = 5.1, 3.6 Hz, 1H), 6.89 (dd, J = 3.6, 1.2 Hz, 1H), 6.98 (d, J = 5.1 Hz, 1H), 7.14 (dd, J = 5.1, 1.2 Hz, 1H), 7.14 (d, J = 7.9 Hz, 4H), 7.24 (d, J = 5.1 Hz, 1H), 7.40 (d, J = 7.9 Hz, 4H). ^{13}C NMR ($CDCl_3$) δ 1.7, 21.6, 124.5, 125.7, 127.1, 127.6, 128.4, 133.5, 134.8, 135.0, 136.1, 137.2, 139.4, 144.9; ^{29}Si NMR ($CDCl_3$) δ −25.1, 9.9. Exact MS Calc. for $C_{22}H_{18}S_2Si$: 374.0608. Found: 374.0618.

Table 1
Synthesis of polymer **2**[a]

Run	Electrolyte amt (M)	Electrical charge (F/mol)	Yield[b] (%)	Mw (Mw/Mn)	UV λ_{max} (nm)
1	0.1	0.5	9[c]	2700 (1.1)	480
2	0.1	1.0	35[d]	4400 (1.1)	490
3	0.1	1.5	60	4800 (1.2)	487
4	0.1	2.0	70	8400 (1.6)	469
5	0.1	2.5	44	17800 (2.5)	449
6	0.05	2.0	39	7500 (1.2)	424
7	0.2	2.0	79	6300 (1.7)	487
8[e]	0.1	2.0	65	5600 (1.3)	442
9[f]	0.1	2.0	55	9000 (1.4)	450

[a] Compound **1** (622 mg, 1.2 mmol) was electrolyzed on a Pt plate electrode in 200 mL of 0.1 M Et_4NBF_4/AN, at a constant applied potential of +0.92 vs. Ag/Ag^+.

[b] Calculated by assuming that the polymer has ideal poly(dithienosilole) structure shown in Scheme 1.

[c] Compounds **1** (3%), **3** (13%), and **4** (9%) were detected by GC analysis of the reaction mixture.

[d] Compounds **3** (6%) and **4** (9%) were produced.

[e] With the applied potential of +0.85 V vs. Ag/Ag^+.

[f] Bu_4NBPh_4 was used as the supporting electrolyte.

3. Results and discussion

3.1. Anodic polymerization of *1*

When DTS **1** was subjected to anodic oxidation in AN containing 0.1 M of Et_4NBF_4 at a constant potential of +0.92 V vs. Ag/Ag^+, corresponding to the anodic peak potential of **1** in the CV, polymer **2** was obtained as the red brown solids. Table 1 summarizes yields, molecular weights, and UV absorption λ_{max} of polymer **2**, depending on the electrical charge. As presented in Table 1, yields and molecular weights of **2** increased as increasing the electrical charge. UV λ_{max} of **2** moved to lower energies along the electrical charge up to 1.0 F/mol (runs 1 and 2), but further electrolysis led to high-energy shifts of λ_{max} (runs 3–5). This may be understood by decomposition of the dithienosilole rings competing the polymerization. The structure of polymer **2** was verified by IR and NMR spectroscopy. The ^{1}H NMR spectra showed broad and multiple signals of trimethylsilyl, tolyl, and thiophene ring protons, together with unidentified ones with low intensities. The integration ratios of trimethylsilyl and tolyl methyl protons indicated that the group ratio of $Si(p\text{-}Tol)_2/SiMe_3$ increased from 2.8 (run 1) to 5.0 (run 5) as increasing the electrical charge. These values are too small to assign

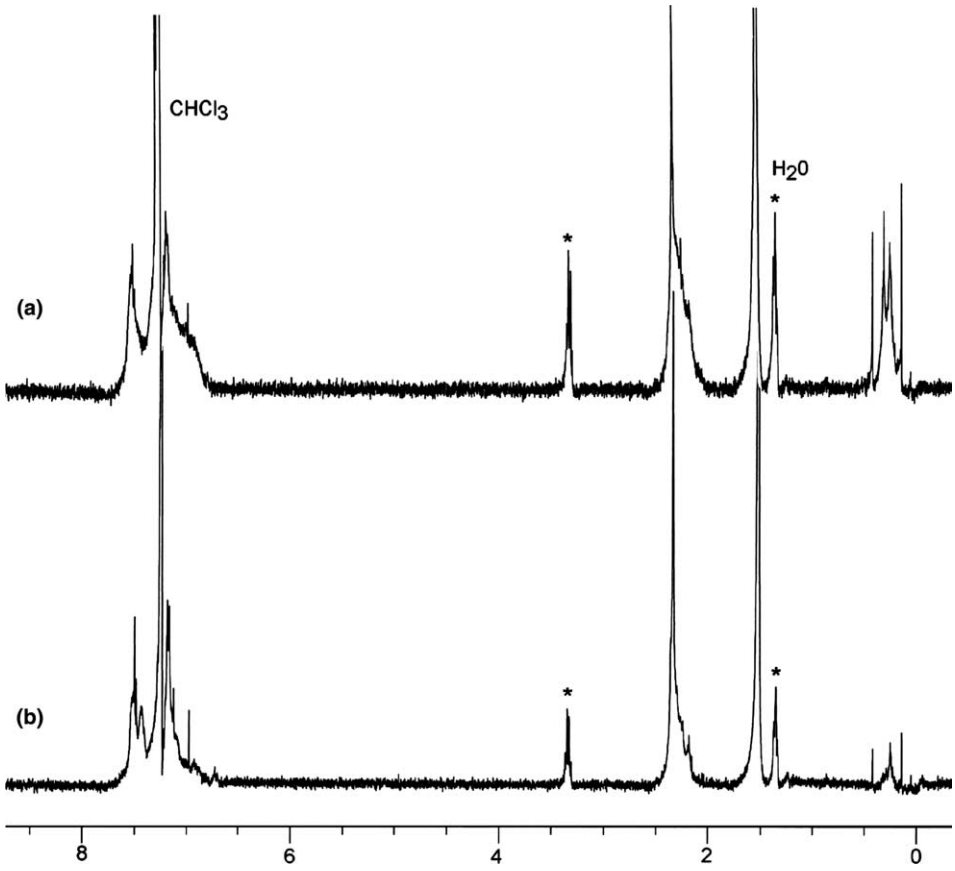

Fig. 1. ^{1}H NMR spectra of polymer samples **2** obtained from (a) run 5 and (b) run 7 in Table 1. Asterisks indicate the signals, probably due to Et_4NBF_4.

the $SiMe_3$ signals only as those of the terminal groups, as shown in Fig. 1(a). Furthermore, the integration ratios of ring protons/tolyl methyl protons ranged from 1.5 to 1.6 that were a little smaller than the calculated value (10/6 = ca. 1.7) based on the ideal structure shown in Scheme 1. Presumably, $SiMe_3$ fragment once formed added to the polymer chain, to an extent, which would be responsible for the blue shifts of the UV λ_{max} along with increasing the electrical charge. IR spectra of the polymer samples always revealed an absorption band assignable to Si–O stretching frequencies at about 1100 cm^{-1}, although the intensity was rather low. At the early stage of the electrolysis (runs 1 and 2), desilylated products **3** and **4** (Chart 1) were separated from the reaction mixtures. No volatile products arising from silole Si–C bond cleavage were detected in the mixtures, indicating that such cleavage was not important, at least, at low electrical charge. In further electrolysis, however, trace amounts of compounds **5** and **6** (see Chart 1) were found to be formed, but the routes to these products are unclear.

The concentration of supporting electrolyte Et_4NBF_4 affected the results. Thus, as shown in Table 1, runs 4, 6, and 7, electrolysis of **1** with the higher concentration of the electrolyte afforded polymer **2** with the longer λ_{max}.

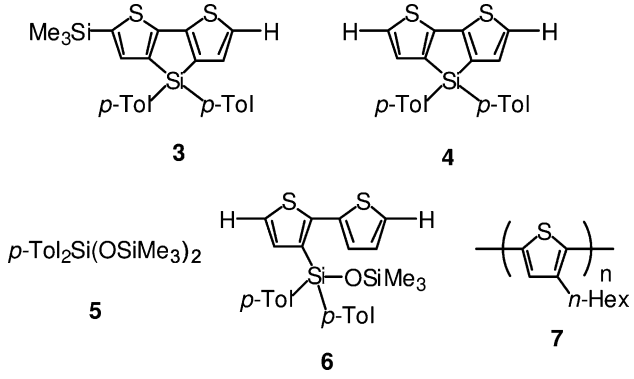

Chart 1. Structures of compounds **3**–**7**.

In accordance with this, the high proton integration ratio of $Si(p\text{-Tol})_2/SiMe_3$ = 9.1 was obtained for the polymer obtained from runs 7 (Fig. 1(b)), indicating that the addition of $SiMe_3$ fragment was suppressed remarkably by increasing the concentration of Et_4NBF_4 that would capture the reactive $SiMe_3$ species as electrochemically inert $FSiMe_3$. The integration ratio of ring protons/tolyl methyl protons of the polymer from run 7 was 1.7, consistent with the ideal poly(dithienosilole) structure shown in Scheme 1. Carrying out the electrolysis at

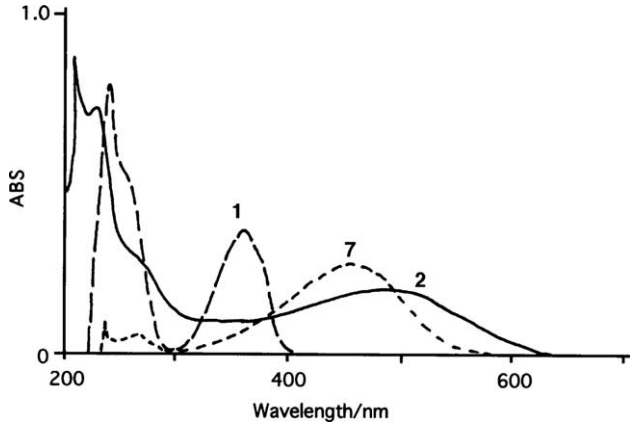

Fig. 2. UV spectra of DTS **1**, polymer **2**, and polymer **7** in THF.

slightly lower potential (+0.85 V vs. Ag/Ag^+) resulted in a blue shift of the polymer λ_{max} (see runs 4 and 8). Using Bu_4NBPh_4 as the supporting electrolyte again caused a blue shift (run 9).

Fig. 2 represents the UV spectra of the starting monomer **1**, polymer **2** from run 7, and poly(3-hexylthiophene) (**7** in Chart 1, regio regularity: head to head content >97%). As can be seen in Fig. 2, the absorption of **2** exhibits longer λ_{max} and λ_{edge} than those of **1** and **7**. Broadening of absorption band of polymer **2** is presumably due to the random structure arising from partial decomposition of the dithienosilole rings. Polymer **2** was found to be electrochemically active and a cyclic voltammogram (CV) of its film on an ITO electrode revealed irreversible oxidation peaks at +0.5 and +0.8 V vs. Ag/Ag^+. No cathodic counter parts were observed, in marked contrast to polythiophene **7** that showed a reversible CV profile. The oxidation peaks of **7** appeared at +0.2 and +0.6 V vs. Ag/Ag^+ in its CV, indicating the lower lying HOMO energy level of **2** than **7**. Taking the red shifted UV λ_{max} of **2** into account, it seems likely that polymer **2** has the LUMO at lower energy as compared with **7**.

In order to elucidate the electronic states of **2**, we carried out molecular orbital (MO) calculations for model oligomers **2′** and **7′** shown in Fig. 3. For the calculations, the geometries were optimized at the RHF/6-31G level and the energy calculations were performed at the RHF/6-31G** level [10]. All the optimized geometries of the oligomers exhibit high coplanarity of the thiophene rings. Fig. 3 represents relative HOMO and LUMO energy levels derived from the calculations, suggesting that DTS oligomers **2′** possesses both HOMO and LUMO at lower energies than those of thiophene oligomers **7′**. The differences in LUMO energy levels were predicted to be larger than in HOMOs, giving rise

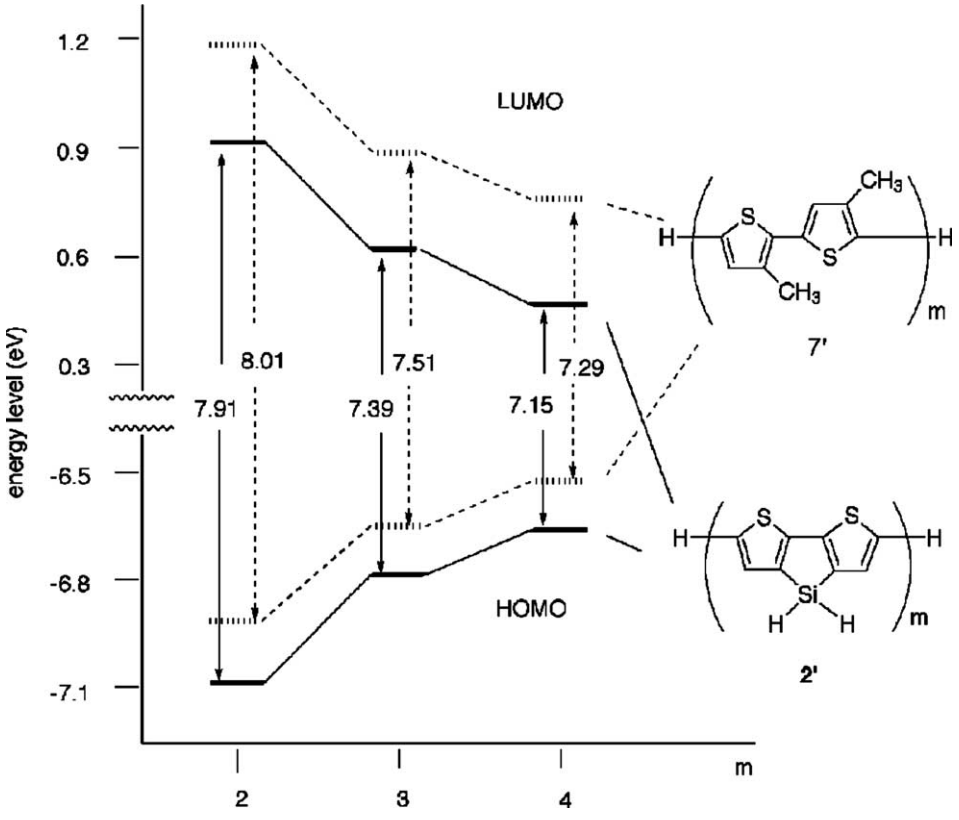

Fig. 3. Relative HOMO and LUMO energy levels of model compounds, **2′-m** and **7′-m**, derived from MO calculations at the level of RHF/6-31G// RHF/6-31G**.

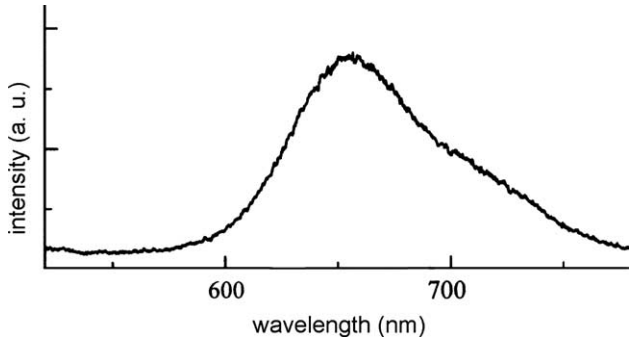

Fig. 4. Emission spectrum of a spin-coated film of polymer **2** obtained from run 7 in Table 1.

to smaller HOMO–LUMO energy gaps of **2′** relative to **7′**.

3.2. Applications of polymer **2** to semi-conducting and electroluminescent materials

When a spin coated film of **2** obtained from run 7 was doped with $FeCl_3$ vapor, the film became semi-conducting with a conductivity of 2.5×10^{-5} S/cm. Rather low conductivity of **2** may be due to the substituents on the silole silicon atom, which cover the polymer chain to prevent smooth carrier hopping through interchain interactions in the solid state. Structure irregularity arising from decomposition of the silole rings may be also responsible for the low conductivity.

Polymer **2** exhibited strong photoluminescnece (PL) in solutions as well as in the solid states (Fig. 4), whose quantum yield was determined to be $\Phi = 0.12$ in THF (1.0×10^{-5} g/L), relative to 9,10-diphenylanthracene solution as a standard. We next examined polymer **2** from run 7, with respect to its emitting properties in an electroluminescent (EL) system. Thus, as shown in Fig. 5(a), a device with the structure of ITO/polymer **2** (30–40 nm)/Alq3 (50 nm)/ Mg:Ag (10:1), where ITO and Alq3 were indium tin oxide and tris(8-hydroxyquinoline)aluminium, respectively, emitted a light by applying the bias voltage to reach the maximum luminance of 370 cd/m^2 at 17.5 V. The current density at 17.5 V was 460 mA/cm^2 (Fig. 5(b)). The device emitted a yellowish brown light up to ca. 18 V, while the color changed to red by applying higher voltage. This process was irreversible and the device, to which high voltage had been once applied, emitted a red light even from low voltage region. As shown in Fig. 5(c), the EL spectrum at 17 V consists of two maxima at 536 and 656 nm. The former may be ascribed to Alq3 emission, while the latter may originate form the polymer layer. At 23 V, however, the spectrum revealed only one maximum due to the polymer emission. Presumably, morphological changes in the polymer film and/or in the polymer–Alq3 interface occurred by applying high voltage, although we could not obtain any evidences to support this. A single layer device, ITO/**2** (50–100 nm)/ Mg:Ag (10:1), also emitted a red light, although the maximum luminance was only 0.42 cd/m^2 at the applied

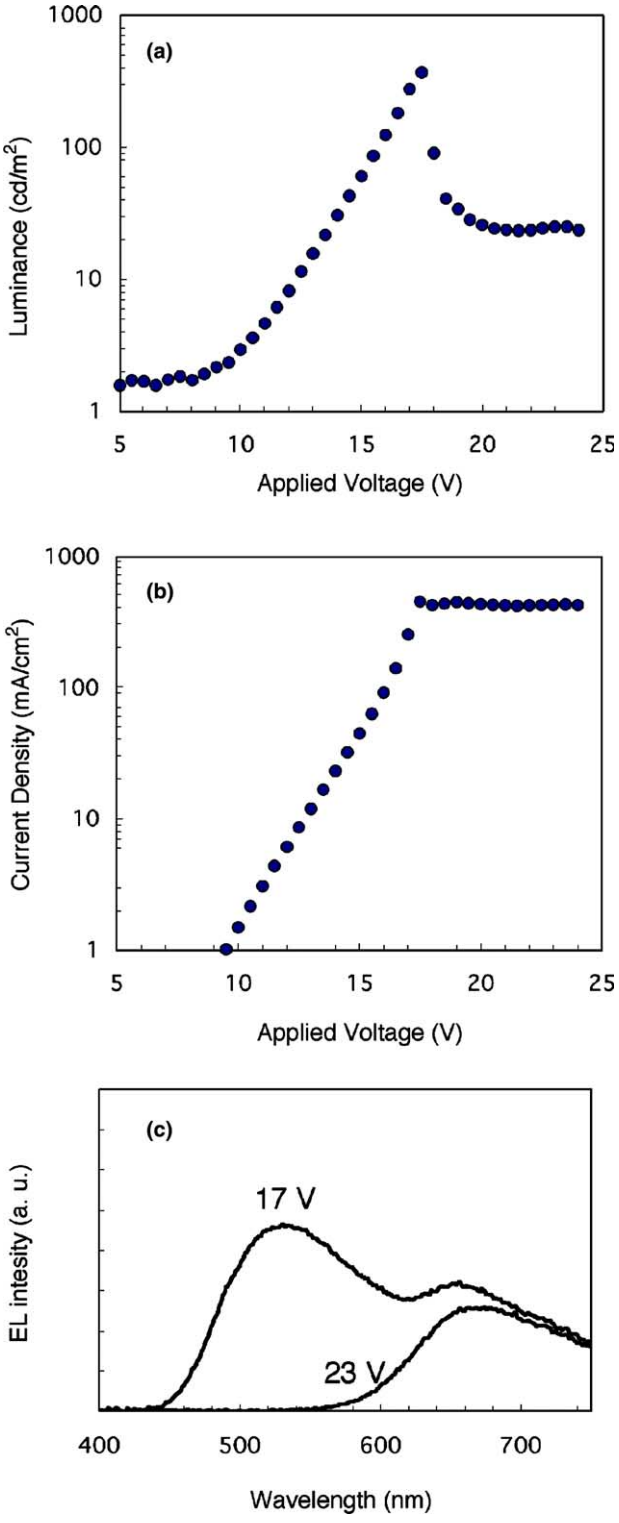

Fig. 5. (a) *L–V* and (b) *I–V* plots of EL device, ITO/polymer **2**/Alq3/ Mg:Ag. (c) EL spectra from the device at 17 and 23 V.

voltage of 32.0 V. The current density at this voltage was 37.5 mA/cm^2.

In conclusion, we synthesized novel silole-containing polymer **2** that may be used as emitting materials in EL device systems. The studies also indicated that DTS unit seems to be potentially useful as a component of novel conjugated polymers with small band gaps.

Acknowledgments

This work was supported by the Ministry of Education, Culture, Supports, Science and Technology (Grant-in-Aid for Scientific Research, No. 16350102). We thank Tokuyama Co. Ltd. and Sankyo Kasei Co. Ltd. for financial support.

References

[1] (a) S. Yamaguchi, K. Tamao, J. Chem. Soc., Dalton Trans. (1998) 3693;
(b) S. Yamaguchi, K. Tamao, J. Organomet. Chem. 611 (2000) 5.
[2] (a) M. Uchida, T. Izumikawa, T. Nakano, S. Yamaguchi, K. Tamao, Chem. Mater. 13 (2001) 2680;
(b) J. Luo, Z. Xie, W.Y. Lam, L. Cheng, H. Chen, C. Qiu, H.S. Kwok, X. Zhan, Y. Liu, D. Zhu, B.Z. Tang, Chem. Commun. (2001) 1740;
(c) A. Adachi, H. Yasuda, T. Sanji, H. Sakurai, K. Okita, J. Lumin. 87–89 (2000) 1174;
(d) J. Chen, C.C.W. Law, J.W.Y. Lam, Y. Dong, S.M.F. Lo, I.D. Williams, D. Zhu, B.Z. Tang, Chem. Mater. 15 (2003) 1535.
[3] (a) S. Yamaguchi, K. Tamao, J. Organomet. Chem. 653 (2002) 223;
(b) M.S. Liu, J. Luo, A.Y.-K. Jen, Chem. Mater. 15 (2003) 3496;
(c) G. Zhang, J. Ma, Y. Jiang, Macromolecules 36 (2003) 2130;
(d) S. Yamaguchi, T. Goto, K. Tamao, Angew. Chem., Int. Ed. 39 (2000) 1695.
[4] S. Yamaguchi, R.-Z. Jin, Y. Itami, K. Tamao, J. Am. Chem. Soc. 121 (1999) 10420.
[5] (a) Z.-R. Zhang, J.Y. Becker, R. West, J. Electroanal. Chem. 507 (2001) 49;
(b) A. Dhiman, Z.-R. Zhang, R. West, J.Y. Becker, J. Electroanal. Chem. 569 (2004) 15.
[6] Y. Lee, S. Sadki, B. Tuie, J.R. Reynolds, Chem. Mater. 13 (2001) 2234.
[7] J. Ohshita, M. Nodono, H. Kai, T. Watanabe, A. Kunai, K. Komaguchi, M. Shiotani, A. Adachi, K. Okita, Y. Harima, K. Yamashita, M. Ishikawa, Organometallics 18 (1999) 1453.
[8] J. Ohshita, H. Kai, A. Takata, T. Iida, A. Kunai, N. Ohta, K. Komaguchi, M. Shiotani, A. Adachi, K. Sakamaki, K. Okita, Organometallics 20 (2001) 4800.
[9] J. Ohshita, H. Kai, T. Sumida, A. Kunai, A. Adachi, K. Sakamaki, K. Okita, J. Organomet. Chem. 642 (2002) 137.
[10] GAUSSIAN 98, Revision A.9, Gaussian, Inc., Pittsburgh, PA.